

R-VA A NEW FRACTAL PARAMETER FOR GRAYSCALE IMAGE CHARACTERIZATION

Mircea-Sebastian Serbanescu, Iancu Emil Plesea

Department of Pathology, University of Medicine and Pharmacy of Craiova

Corresponding author: Mircea-Sebastian Serbanescu, mircea_serbanescu@yahoo.com

ABSTRACT: Computing the fractal dimension (FD) of a grayscale image is not an easy task. We propose a new method for estimating the FD of a grayscale image, defined as the mean ratio between volume and amplitude (R-VA) at different image scales. The proposed algorithm is compared with a standard box-counting algorithm (applied to binarized images) on two image datasets: a texture dataset and a prostate cancer dataset (with Gleason grading labeled images). Results show that R-VA algorithm has better discriminating capabilities than the standard box-counting algorithm on both datasets.

KEYWORDS: fractal dimension, ratio between volume and amplitude, R-VA, grayscale images, prostate cancer, Gleason grading

1. INTRODUCTION

A fractal dimension (FD) is a ratio that provides a statistical index of complexity, comparing the way details of a pattern change along with the measuring scale [***15a].

The use of FD in the medical field is widely spread, ranging from radiology[LG09], where the images are native grayscale images, to pathology [G+14],[Lan96] where the images are fully colored. FD in medical field is used as a feature for describing a given image or part of an image rather than showing a precise value for a known fractal, thus its discrimination capability is its most important characteristic.

The computation of grayscale image fractal dimension is not an easy task. The basic box-counting algorithm is widely used because it is easy to implement and is as simple as counting the boxes needed for covering an object in a binary image at different scales (box size). The problem with the basic box-counting algorithm is that it is applied only to binary images, thus one needs a binarization method to convert a grayscale image to its binary representation (thresholding, edge detection, etc). The chosen method or threshold for binarization usually is empirically selected and there is little to say in favor of the optimum.

In this article we propose a new parameter for grayscale image description, represented as the ratio between volume and amplitude (R-VA) in different image scales, having its origin in a similar parameter

used in signal analysis [Tar97]. To confirm its discrimination capabilities we compare our results with the results from a standard box-counting algorithm, on two image datasets, a texture dataset and a pathology dataset with Gleason grading patterns of prostate carcinoma.

2. MATERIALS AND METHODS

In this section we describe the two datasets, we present the new algorithm, and the way we compare it with the standard box-counting algorithm, evaluating its results on in-class and inter-class variability.

2.1. Datasets

2.1.1. The texture dataset

The first dataset used is the KTH-TIPS - a texture dataset with 10 classes of real images (Sandpaper, Crumpled aluminium foil, Styrofoam, Sponge, Corduroy, Linen, Cotton, Brown bread, Orange peel, Cracker) each having 81 samples per class. The dataset provides variation in scale as well as variation in pose and illumination. A detail description of the dataset can be found at [***15b] and samples are presented in Figure 5.

2.1.2. The prostate cancer dataset

The second dataset consists of a selection of 299 labeled (Gleason grading[Gle77], [A+03]) digital images of the fibrillary tumoral network, acquired from Gömöri stained sections of prostate carcinoma. A more detailed description of the dataset can be found in [S+12], [P+13] and samples are presented in Figure 6.

2.2 Algorithms

Starting from the general formula of the FD, consider e as the scale, $N(e)$ as the detail characterization on scale e , FD as the fractal dimension, and C as a constant number, let:

$$N(e) = C * e^{FD}$$

A numerical approximation of the FD is obtained:

$$FD = \text{slope} \left(\frac{\text{Log}(N(e))}{\text{Log}(e)} \right)$$

2.2.1. Standard box-counting algorithm

We obtain the standard box-counting algorithm by computing $N(e)$ as the number of boxes required to cover the structures in a binary image with scale e :

- (1) Set the box size “ e ” to the size of the image.
- (2) Compute (e) , which corresponds to the number of boxes of size “ e ” which contains at least one object pixel.
- (3) If $e > 1$ then $e = e/2$ and repeat step (3).
- (4) Compute the points $\log(N(e)) \times \log(1/e)$.
- (5) Use the least squares method to fit a line to the points.
- (6) The returned FD is the slope of the line.

2.2.2. R-VA algorithm

By computing $N(e)$ as the average ratio between the actual volume and the actual amplitude (power 3, in order for the final number to be adimensional) of a grayscale image split in images of size $e \times e$, we obtain the R-VA algorithm:

- (1) Set the grid size “ e ” to the size of the image.
- (2) Compute (e) , which corresponds to mean Volume/Amplitude value of the image scanned with the grid of size e .
- (3) If $e > 1$ then $e = e/2$ and repeat step (3).
- (4) Compute the points $\log(N(e)) \times \log(1/e)$.
- (5) Use the least squares method to fit a line to the points.
- (6) The returned FD is the slope of the line.

2.3. Image preprocessing

2.3.1 The texture dataset

Preprocessing of the texture dataset implies cropping square images of 113x113 pixels from the original images and scaling them to 128x128 pixels (Figure 1). Images of 113x113 pixels represent the largest square that could be fitted in all the dataset images.

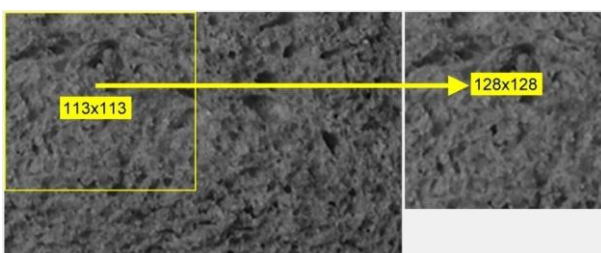


Figure 1. Preprocessing of the images in the texture dataset, the largest square available in all images (113x113 pixels) is scaled to 128x128 pixels (size is power of 2)

2.3.2. The prostate cancer dataset

Preprocessing of the prostate cancer dataset implies cropping square images of 960x960 pixels from the original images, and scaling them to 512x512 pixels, then transforming them to grayscale images by averaging each color channel (Figure 2). Images of 960x960 pixels represent the largest square that could be fitted in all the dataset images.

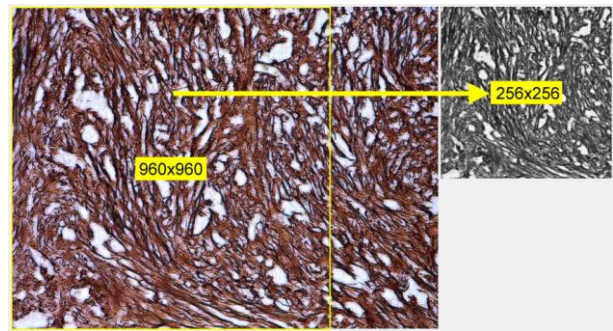


Figure 2. Preprocessing of the images in the prostate cancer dataset, the largest square available in all images (960x960 pixels) is scaled to 512x512 pixels (size is power of 2)

2.4. Evaluation

The aim of the evaluation is to present the inter- and in-class variation of the results of our proposed R-VA algorithm, when compared to the results from the standard box-counting algorithm. The inter-class variation should be as large as possible, while the in-class variation should be as small as possible.

The score for inter-class variation is statistically calculated as the different mean values of each data class tested against all the other classes (student t-test, two tails, assuming unequal variations).

The maximum possible score for the texture dataset is 45 and for the prostate cancer dataset is 28.

The in class variation is assessed as the average standard deviation of all classes. The smaller the in-class variation is, the better the result is considered.

2.4.1 Texture dataset evaluation

For the standard box-counting algorithm the images are binarized with two techniques: thresholding and edge detection. For the best threshold estimation the images are binarized with a variable threshold ranging from the 1st to the 99th percentile of each image histogram. In order to find the best edge detector, six different methods are tested: Sobel, Perwitt, log, zerocross, Canny, Roberts.

The R-VA algorithm is applied directly to the grayscale images.

2.4.2. Prostate cancer dataset evaluation

For the standard box-counting algorithm the images are binarized with the best threshold value and the best edge detection method, obtained from the texture dataset evaluation.

The R-VA algorithm is applied directly to the grayscale images.

3. RESULTS

3.1. Texture dataset

The scores for inter-class evaluation of the standard box-counting algorithm, applied to threshold images with variable threshold between 2nd and 99th percentile of each image histogram, are presented in Figure 3. The best score is obtained at the 80th percentile threshold and it is 35, out of a maximum of 45.

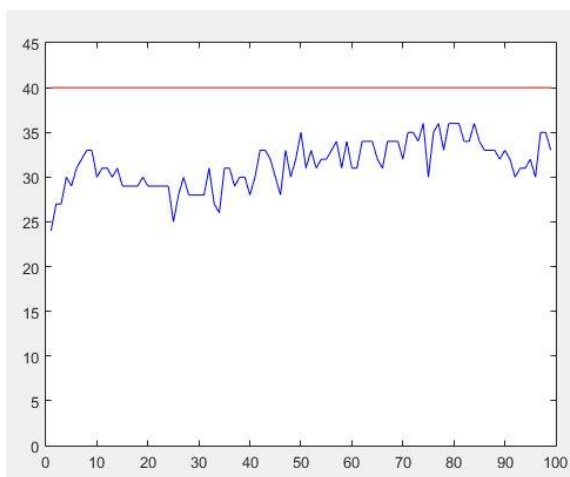


Figure 3. Results of the box-counting algorithm inter-class score with images thresholded with percentile 2 to 99 of each image histogram (blue) and inter-class score for the R-VA algorithm (red)

The scores of the standard box-counting algorithm applied to the binary images resulted from the edge detection algorithms are presented in figure 4. The best score obtained is 39 out of 45, obtained using the Roberts edge detector method.

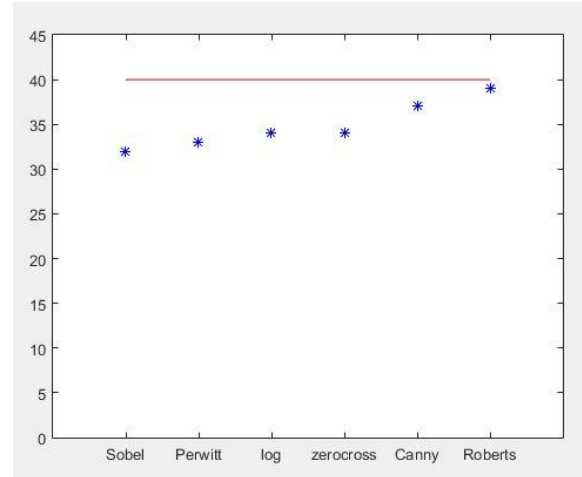


Figure 4. Results of the box-counting algorithm inter-class score with images binarized with edge detector algorithms (blue) and inter-class score for the R-VA algorithm (red)

The score for the R-VA algorithm is 40 out of a maximum of 45. The score is marked with a red line in Figures 3 and 4.

In-class variability is 0.026 for the best (80th) percentile threshold, 0.103 for the Roberts edge detector method and 0.031 for R-VA algorithm.

Figure 5 shows two images and the corresponding binary images obtained by using the 80th percentile threshold and the Roberts edge detector method. Table 1 shows the computed values for each class, for the standard box-counting algorithm (applied to the binary images obtained by thresholding and edge detection for the R-VA algorithm).

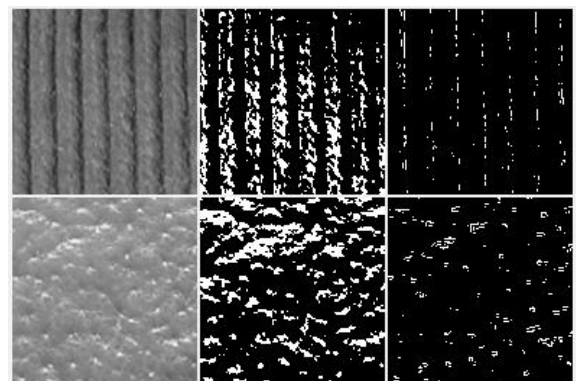


Figure 5. Texture dataset example: two sample images (left) with corresponding 80th percentile threshold image (center) and Roberts edge detector result (right)

3.2. Prostate cancer dataset

The calculated score of the standard box-counting algorithm applied to thresholded (80th percentile) images is 15 out of 28, for the Roberts edge detector method the score is 17, and for the R-VA algorithm the calculated score is 20.

In-class variability is found to be 0.020 for the 80th percentile threshold, 0.109 for the Roberts edge detector method and 0.021 for R-VA algorithm.

Figure 6 shows images and their corresponding binary images obtained by using the 80th percentile threshold and the Roberts edge detector method for

two image samples. Table 2 shows the computed values for each class, for the standard box-counting algorithm applied to the binary images obtained by thresholding and by edge detection, as well as for the R-VA algorithm.

Table 1. Results (mean and standard deviation) obtained with the standard box-counting algorithm, with images binarized with the 80th percentile, the Roberts edge detector method and with the R-VA algorithm on the texture dataset

| | Standar box-counting algorithm Thresholded with the 80 th percentile Mean/standard deviation | | Standar box-counting algorithm Thresholded with Roberts edge detector Mean/standard deviation | | R-VA algorithm Applied directly to grayscale images Mean/standard deviation | |
|-------------------------|---|-------|---|-------|---|-------|
| | Sandpaper | 1.659 | 0.027 | 1.210 | 0.179 | 1.791 |
| Crumpled aluminium foil | 1.674 | 0.020 | 1.112 | 0.081 | 1.880 | 0.040 |
| Styrofoam | 1.676 | 0.028 | 1.011 | 0.205 | 1.894 | 0.020 |
| Sponge | 1.708 | 0.042 | 0.641 | 0.273 | 1.923 | 0.032 |
| Corduroy | 1.680 | 0.023 | 1.056 | 0.061 | 1.844 | 0.027 |
| Linon | 1.718 | 0.028 | 1.021 | 0.235 | 1.897 | 0.024 |
| Cotton | 1.662 | 0.025 | 1.186 | 0.076 | 1.915 | 0.029 |
| Brown bread | 1.699 | 0.028 | 1.030 | 0.068 | 1.897 | 0.033 |
| Orange peel | 1.690 | 0.020 | 1.115 | 0.054 | 1.876 | 0.028 |
| Cracker | 1.710 | 0.022 | 1.139 | 0.077 | 1.857 | 0.016 |

Table 2. Results (mean and standard deviation) obtained with the standard box-counting algorithm, for images binarized with the 80th percentile, the Roberts edge detector method, and with the R-VA algorithm on the prostate cancer dataset. There were no images labeled with Gleason pattern 1 in the dataset

| | Standar box-counting algorithm Thresholded with the 80 th percentile Mean/standard deviation | | Standar box-counting algorithm Thresholded with Roberts edge detector Mean/standard deviation | | R-VA algorithm Applied directly to grayscale images Mean/standard deviation | |
|--------------------|---|-------|---|-------|---|-------|
| | Gleason pattern 1 | - | - | - | - | - |
| Gleason pattern 2 | 1.760 | 0.018 | 1.320 | 0.093 | 1.908 | 0.025 |
| Gleason pattern 3a | 1.750 | 0.022 | 1.339 | 0.091 | 1.893 | 0.020 |
| Gleason pattern 3b | 1.760 | 0.018 | 1.267 | 0.107 | 1.905 | 0.023 |
| Gleason pattern 3c | 1.748 | 0.021 | 1.338 | 0.082 | 1.889 | 0.031 |
| Gleason pattern 4a | 1.754 | 0.022 | 1.282 | 0.125 | 1.904 | 0.012 |
| Gleason pattern 4b | 1.735 | 0.027 | 1.329 | 0.082 | 1.912 | 0.012 |
| Gleason pattern 5a | 1.750 | 0.010 | 1.262 | 0.168 | 1.866 | 0.012 |
| Gleason pattern 5b | 1.759 | 0.023 | 1.182 | 0.126 | 1.907 | 0.033 |

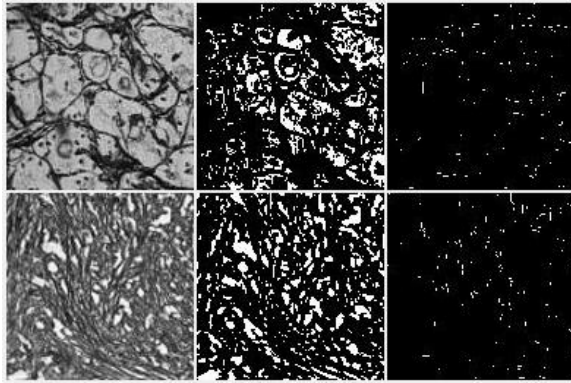


Figure 6. Prostate Cancer dataset example: two sample images (left) with corresponding 80th percentile threshold image (center) and Roberts edge detector result (right). Image on the top is Gleason pattern 2 and image on the bottom is Gleason pattern 5b

4. DISCUSSION

Taking into consideration the results of the texture dataset we can state that the binarization method influences the final results. Figure 3 shows the largest variation in inter-class discrimination score for the threshold method – the lowest score is 24/48 while the highest is 36/48. For the edge detection method the discrimination score has lower variability and tends to be higher than the threshold method – the lowest score is 32 (Sobel), while the highest score is 39 (Roberts). We can say that using the edge detection method is better than using a threshold method, but this might be a local dataset optimal – we have no formal support for this affirmation. The result of the R-VA algorithm (40) is better than any of the results from the standard box-counting algorithm. In-class variability tends to have better results (lower variation) for the R-VA algorithm – 0.031 – than for the box-counting algorithm on binarized images with the Roberts edge detector method – 0.130 – and lower results compared with the 80th percentile threshold binarized images – 0.026.

Taking in consideration the results of the prostate cancer dataset, the inter-class scores are better for the R-VA algorithm (9/28) than the scores of the box-counting algorithm (4/28 for the 80th percentile threshold and 7/28 for the Roberts edge detector method). The in-class variation has a better result for the R-VA algorithm, mean standard deviation is 0.021, while for the box-counting algorithm the mean standard deviation is 0.020 for the 80th percentile threshold, and 0.109 for the Roberts edge detector method.

The average scores of the prostate cancer dataset are lower than the ones from the texture dataset. A possible explanation is that while the images from the texture dataset come from the same object, the

images from the prostate cancer come from different sources (patients).

The FD for gray level images is measured considering the gray level surface of the images. There are other methods for estimating the FD of a grayscale image. In [P+84] the 3D surface of the image is covered by a “digital blanket” and the quantification of the size of the blanket is used to obtain the FD - blanket method. In [Pen84] the Fourier power spectrum is used to compute the FD, the image intensity surface being considered a Brownian function. The closest approach to our algorithm is the differential box-counting algorithm [SC94] which takes into consideration the maximum and minimum grey-level values of the boxes, in a 3D space. All the other methods for computing the FD of a grayscale image have higher computational complexity when compared with the R-VA.

5. CONCLUSION

We have developed a new parameter to characterize grayscale medical images, with superior discriminating results when compared to a standard box-counting algorithm applied to the binarized version of the images. Our parameter is a less computationally intensive algorithm when compared to other methods of computing FD on grayscale images. Its main advantage is that it is applied directly to grayscale images without an intermediary step of binarization.

ACKNOWLEDGEMENT

This paper was published under the frame of European Social Found, Human Resources Development Operational Program 2007-2013, project no. POSDRU/159/1.5/136893.

REFERENCES

- [A+03] **M. B. Amin, D. Grignon, P. A. Humphrey, J. R. Srigley** - *Gleason Grading of Prostate Cancer: A Contemporary Approach*, in Lippincott Williams & Wilkins, New York, 2003
- [Gle77] **D. F. Gleason** - *The veteran's administration cooperative urologic research group: Histologic grading and clinical staging of prostatic carcinoma*, in *Urologic Pathology: The Prostate*, M. Tannenbaum Ed. Lea and Febiger, Philadelphia, PA, pp. 171-198, 1977
- [G+14] **D. I. Gheonea, C. T. Streba, C. C. Vere, M. Serbanescu, D. Pirici, M. Comanescu, L. A. Streba, M. E.**

- Ciurea, S. Mogoanta, I. Rogoveanu** - *Diagnosis system for hepatocellular carcinoma based on fractal dimension of morphometric elements integrated in an artificial neural network*, in Biomed Res Int, 2014
- [Lan96] **G. Landini** - *Applications of fractal geometry in pathology* - in *Fractal Geometry in Biological Systems: An Analytical Approach*, P. M. Iannaccone and M. Khokha, Eds. CRC Press, Boca Raton, pp.205-246, 1996
- [LB09] **R. Lopes, N. Betrouni** - *Fractal and multifractal analysis: a review*, in *Med Image Anal.*, vol. 13, issue 7, pp.634-649, August 2009
- [Pen84] **A. Pentland** - *Fractal-based description of natural scenes*, in *IEEE Trans. on PAMI*, vol. PAMI-6, issue 6, pp. 661-674, 1984
- [P+13] **I. E. Plesea, A. Stoiculescu, M. Serbanescu, D. O. Alexandru, M. Man, O. T. Pop, R. M. Plesea** - *Correlations between intratumoral vascular network and tumoral architecture in prostatic adenocarcinoma*, in *Rom J MorpholEmbryol*, vol. 54, issue 2, pp. 299–308, 2013
- [P+84] **S. Peleg, J. Naor, R. Hartley, D. Avnir** - *Multiple resolution texture analysis and classification*, in *IEEE Trans. on PAMI*, vol. PAMI-6, issue 6, pp. 518-523, 1984
- [SC94] **N. Sarkar, B. B. Chaudhuri** - *An Efficient Differential Box-Counting Approach to Compute Fractal Dimension of Image*, in *IEEE Trans. on Systems, Man, and Cybernetics*, vol. 24, issue 1, January 1994
- [S+12] **A. Stoiculescu, I. E. Plesea, O. T. Pop, D. O. Alexandru, M. Man, M. Serbanescu, R. M. Plesea** - *Correlations between intratumoral interstitial fibrillary network and tumoral architecture in prostatic adenocarcinoma*, in *Rom J MorpholEmbryol*, vol. 53, issue 4, pp. 941–950, 2012
- [Tar97] **M.T. Tarata** - *The Average Area / Amplitude Ratio (Raa), A Consistent Parameter in the Quantitative Analysis of the Electromyogram*, in *Proceedings of the International Conference on Medical Physics & Biomedical Engineering MPBE'94*, Nikos Milonas, Nicosia, pp. 53-57, May 5-7 1994
- [***15a] Fractal dimension: https://en.wikipedia.org/wiki/Fractal_dimension, Accessed 07 July 2015
- [***15b] The KTH-TIPS image database: <http://www.nada.kth.se/cvap/databases/kth-tips/download.html>, Accessed 07 July 2015